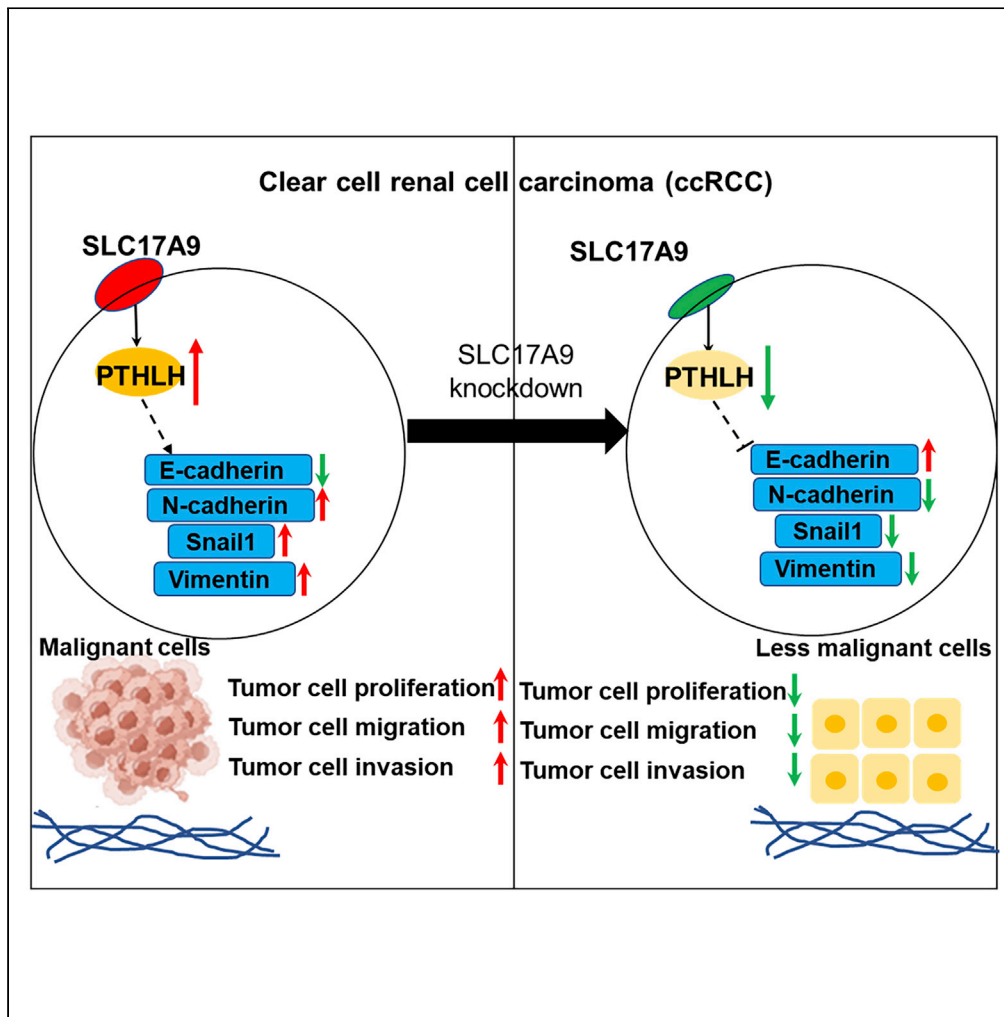# iScience

Article

SLC17A9-PTHLH-EMT axis promotes proliferation and invasion of clear renal cell carcinoma

Weiquan Li, Ning Xu, Xiangui Meng, ..., Bo Hai, Wen Xiao, Xiaoping Zhang

haibo2022@hust.edu.cn (B.H.)
wxuro20@hust.edu.cn (W.X.)
xzhang@hust.edu.cn (X.Z.)

Highlights

SLC17A9 is identified as an unfavorable biomarker for ccRCC

SLC17A9 promotes the progression of ccRCC by upregulating PTHLH-dependent EMT process

SLC17A9 might be positive related to drug resistant of vorinostat

Article

SLC17A9-PTHLH-EMT axis promotes proliferation and invasion of clear renal cell carcinoma

Weiquan Li,[1,2,4] Ning Xu,[3,4] Xiangui Meng,[1,2,4] Hongwei Yuan,[1,2] Tiexi Yu,[1,2] Qi Miao,[1,2] Hongmei Yang,[3] Bo Hai,[1,2,*] Wen Xiao,[1,2,*] and Xiaoping Zhang[1,2,5,*]

SUMMARY

SLC17A9 is a vesicular ATP transport protein that plays an important role in determining cell functions and the onset and progression of different diseases. In this study, SLC17A9 was initially identified as a potential diagnostic and prognostic risk biomarker for clear cell renal cell carcinoma (ccRCC). Then, the aberrant expression levels of SLC17A9 were confirmed in both the cell lines and clinical tissues. Mechanistically, SLC17A9 could upregulate the expression of PTHLH, thus promoting epithelial-mesenchymal transition (EMT) in ccRCC. Functionally, SLC17A9 knockdown inhibited the proliferation, migration, and invasion activity of renal cancer cells, whereas its overexpression led to stronger cell viability and more malignant phenotype *in vitro*. The overexpression of SLC17A9 *in vivo* could significantly contribute to the growth of tumors. Finally, we found that SLC17A9 might be related to the drug resistance of vorinostat. Cumulatively, this study demonstrated that the SLC17A9-PTHLH-EMT axis could promote the progression of ccRCC.

INTRODUCTION

Renal cancer is an epithelial tumor with high global incidence rates in both men and women.[1–3] According to recent statistics, 77,410 new cases of renal cancer and 46,345 associated deaths are estimated in China in 2022.[3] The incidence rate of renal cancer is increasing every year, which may be due to the improvement in medical technology. More than 17% of patients are detected with metastasis at the time of diagnosis.[4,5] Renal cancer is classified into 16 different subtypes based on the 2016 WHO classification, among which clear cell renal cell carcinoma (ccRCC) is responsible for more than 75% of cases and is also one of the highly malignant tumors.[6] Therefore, it is imperative to discover effective tumor markers and the possible mechanisms for ccRCC progression, which can help in the development of new therapeutic drugs.

Solute carrier family 17 member 9 (SLC17A9) encodes a protein that participates in the vesicular nucleotide transport. It has been reported that SLC17A9 could affect cell viability by influencing lysosome dysfunction.[7,8] Although the prognostic value of SLC17A9 has been evaluated in prostate cancer, hepatocellular carcinoma, gastric carcinoma, and colorectal cancer,[9–12] there is still a need to investigate whether SLC17A9 could act as a potential biomarker for ccRCC and elucidate the role of SLC17A9 in promoting tumor progression. As an important transport protein, several drugs targeting SLC17A9 have been investigated for the treatment of steatohepatitis, acute liver injury, type 2 diabetes, and depression.[13–15] This indicates that SLC17A9 could act as a novel drug target for RCC.

Epithelial-mesenchymal transition (EMT) is one of the most complex signaling pathways and hallmarks in different types of cancers.[16] It is believed that EMT plays a significant role in the progression of almost all types of cancer during initiation, invasion, and metastasis. Moreover, it also influences the choice of multiple drug treatment options.[17] E-cadherin (encoded by CDH1) is believed to be a metastatic suppressor in EMT progression. On the contrary, N-cadherin (encoded by CDH2), vimentin (encoded by VIM), and Snail-1 (encoded by SNAI1) are considered to be the positive hallmarks of EMT. However, the influence of SLC17A9 on the EMT in ccRCC has not yet been investigated.

Parathyroid hormone-like hormone (PTHLH), a protein-coding gene encoding parathyroid hormone-related protein (PTHrP), participates in the progression of several diseases. Studies have demonstrated

[1]Department of Urology, Union Hospital, Tongji Medical College, Huazhong University of Science and Technology, Wuhan 430022, China

[2]Shenzhen Huazhong University of Science and Technology Research Institute, Shenzhen 518000, China

[3]Department of Pathogenic Biology, School of Basic Medicine, Tongji Medical College, Huazhong University of Science and Technology, Wuhan 430030, China

[4]These authors contribute equally

[5]Lead contact

*Correspondence: haibo2022@hust.edu.cn (B.H.), wxuro20@hust.edu.cn (W.X.), xzhang@hust.edu.cn (X.Z.) https://doi.org/10.1016/j.isci. 2022.105764

that PTHLH acts as an important EMT upstream regulator.[18,19] Despite all this, there is a need to elucidate the regulation mechanism of PTHLH and prove the role of PTHLH in the promotion of EMT in ccRCC.

This study proved that SLC17A9 may be a novel diagnostic and prognostic biosignature for ccRCC using public sequencing data, clinical tissue samples, gene set enrichment analysis (GSEA), and a series of *in vitro* cellular experiments. The study highlighted that SLC17A9 could influence the EMT signaling pathway by upregulating the expression of PTHLH. Moreover, SLC17A9 might be associated with the activation of T cells and macrophages, and patients with higher SLC17A9 indicated a better response to immunotherapy. Finally, the study predicted potential drugs targeting SLC17A9, which can provide directions for future research.

RESULTS

SLC17A9 was significantly upregulated in ccRCC and associated with different clinical features

The open sequencing data from TCGA-KIRC was used to analyze the SLC17A9 expression levels of normal and RCC tissues and determine the differences of SLC17A9 expression levels at different clinical stages. The results indicated that the expression level of SLC17A9 was much higher in the tumor group irrespective of analysis using paired or unpaired samples (Figures 1A and 1B). Moreover, the expression level of SLC17A9 showed an increasing trend, with a profound increase observed during the clinical stage (Figures 1C–1G). Patients at the advanced stage of the tumor had higher SLC17A9 levels than those at an initial stage, such as T3 versus T1, T4 versus T2, N1 versus N0, M1 versus M0, and so on. The data from the renal cell cancer European cohort (RECA-EU) in ICGC was used for the validation of the aberrant expression of SLC17A9 (Figures 1H and 1I). These results suggested that SLC17A9 might serve as an unfavorable marker for ccRCC and be positively associated with poorer clinical prognosis.

High SLC17A9 expression demonstrated certain diagnostic and prognostic values in ccRCC

The ROC curve is one of the most common detection indicators for disease diagnosis. It was observed that the expression level of SLC17A9 could successfully distinguish tumor group from normal group when TCGA-KIRC and ICGC-RECA-EU data were applied (Figure 2A: AUC = 0.9459, p < 0.0001; 2B: AUC = 0.9228, p < 0.0001). The time-dependent ROC curves indicated that the diagnostic value of SLC17A9 might increase slightly over time (Figure 2C). Kaplan-Meier (KM) curve has been used for evaluating the prognostic value of SLC17A9 for several years. According to the median expression of SLC17A9, the patients in the TCGA-KIRC cohort were divided into two groups. The results indicated that patients in the group having high SLC17A9 expression levels were associated with poor OS and DFS (Figures 2D and 2E). KM curve using E-MTAB-1980data also supported that SLC17A9 was an unfavorable marker for ccRCC (Figure 2F). In addition, prognosis-related nomogram models were constructed by incorporating SLC17A9 and common clinical indicators using TCGA-KIRC data to predict OS and DFS time for each patient (Figures 2G and S1A). In these models, any patient with older age, higher T stage, N stage, distant metastasis, higher G grade, and higher SLC17A9 expression is allocated higher scores and associated with poorer survival time, which is also observed during the clinical diagnosis. To verify these models, the patients were divided into four groups by quartile, and the differences between the predicted probability and the actual probability at 1, 3, and 5 years, were calculated and compared (Figures 2H–2J and S1B–S1D). The predicted curve and the actual curve had a high degree of coincidence. Moreover, the c-index of both the OS model (0.766) and the DFS model (0.821) were larger than 0.71, indicating the credibility of the model. The univariate and multivariate Cox proportional hazard ratio (HR) analyses of OS and DFS were conducted to further elucidate the prognostic value of SLC17A9 (Tables 1 and 2).

SLC17A9 was truly upregulated in ccRCC cell lines and tissues

Although this study had initially demonstrated that SLC17A9 could work as a potential marker for ccRCC using bioinformatics analysis, some experiments were necessary to verify it. The mRNA levels and protein expression levels of SLC17A9 in cell lines were determined by qRT-PCR and western blot (WB), respectively (Figures 3A and 3B). SLC17A9 in OSRC, A498, 786-O, and CAKI cells was significantly upregulated when compared with SLC17A9 in HK2 cells. Because the mRNA and protein levels of SLC17A9 in 786-O and A498 were higher than those in other cell lines, 786-O and A498 were selected for further experiments. Then, the mRNA and protein expression levels of SLC17A9 were detected in paired ccRCC and their adjacent normal tissues (Figures 3C and 3D). SLC17A9 was highly expressed in most tumor tissues. Finally, the
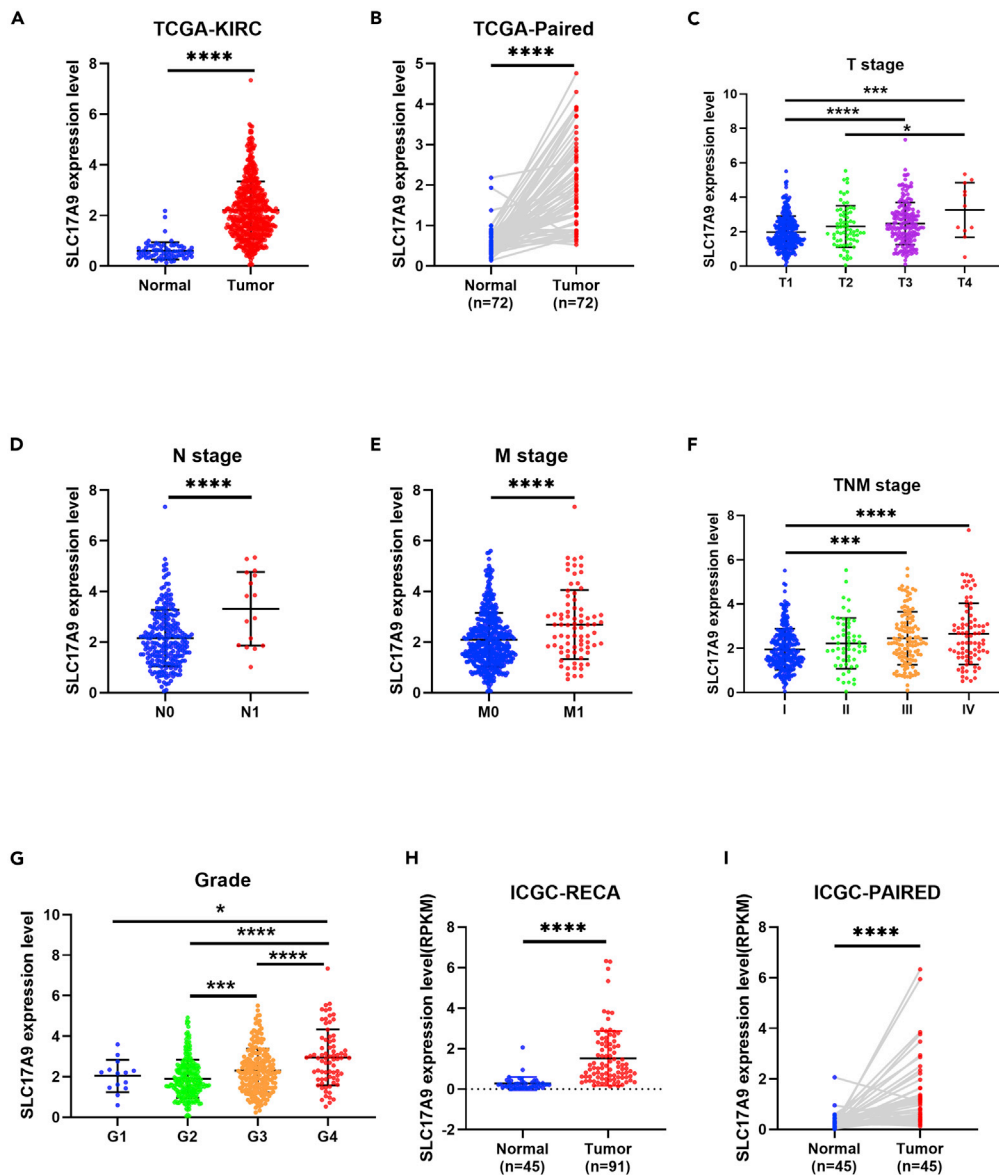
Figure 1. SLC17A9 expression level was upregulated in ccRCC tissues

(A) SLC17A9 mRNA expression levels in the ccRCC tissues were higher than those in the normal tissues in the TCGA cohort.

(B) SLC17A9 expression in normal tissues was lower than that in paired ccRCC tissues.

(C) High expression of SLC17A9 was associated with the T stage and showed an increasing trend.

(D) SLC17A9 expression levels in N0 and N1 stages.

(E) mRNA expression of SLC17A9 in M stage.

(F) SLC17A9 expression levels in different TNM stages in TCGA.

(G) SLC17A9 expression levels in G grade.

(H) SLC17A9 was upregulated in tumor samples compared with normal samples in the ICGC-RECA-EU cohort.

(I) SLC17A9 expression levels in tumor samples were higher than those in paired normal kidney tissues. ****$p < 0.0001$; ***$p < 0.001$; **$p < 0.01$; and *$p < 0.05$. SLC17A9, Solute Carrier Family 17 Member 9; ccRCC, clear cell renal cell carcinoma; KIRC, kidney renal clear cell carcinoma; TCGA, The Cancer Genome Atlas; and ICGC, International Cancer Genome Consortium. Data are represented as mean $\pm$ SD.
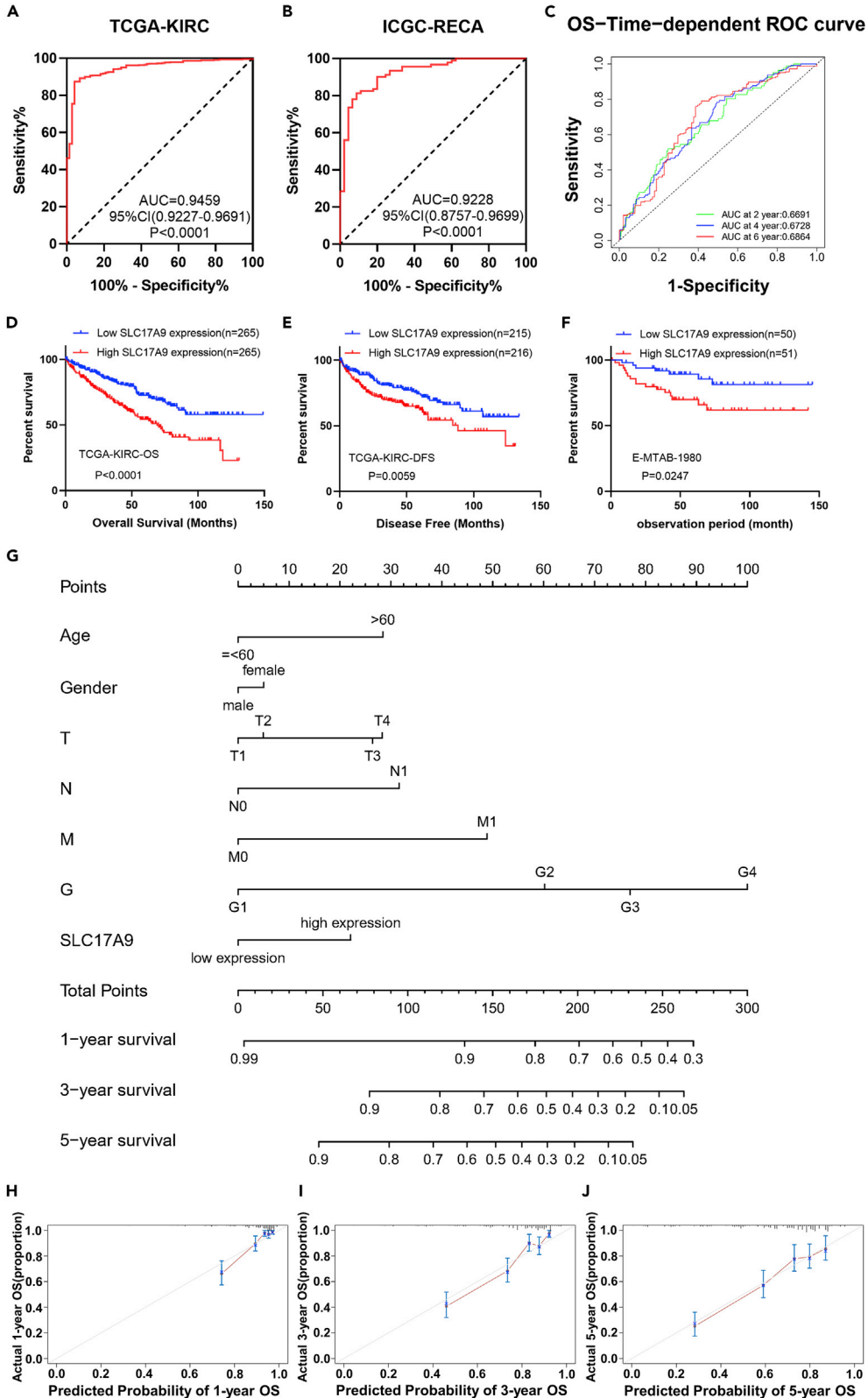
Figure 2. Diagnostic and prognostic values of SLC17A9

(A) SLC17A9 effectively distinguished para-cancer tissues from ccRCC tissues in TCGA-KIRC (AUC = 0.9459, p < 0.0001).

(B) SLC17A9 effectively distinguished para-cancer tissues from ccRCC tissues in ICGC (AUC = 0.9228, p < 0.0001).

(C) Diagnostic value of SLC17A9 for ccRCC patients in TCGA-KIRC increased with time. AUC at 2 years was 0.6691, AUC at 4 years was 0.6728, and AUC at 6 years was 0.6864.

(D) High SLC17A9 expression group had poorer OS than the low expression group in the TCGA cohort, p < 0.0001.

(E) High SLC17A9 expression indicated poorer DFS in the TCGA cohort, p = 0.0059.

(F) Survival analysis of E-MTAB-1980 validation cohort with low SLC17A9 expression group presenting better survival status, p = 0.0247.

(G) Construction of a nomogram for predicting 1-, 3-, and 5-year OS possibilities of individual ccRCC patients.

(H–J) Calibration curves of (H) 1-year, (I) 3-year, and (J) 5-year OS of ccRCC patients. Light-colored diagonal represented predicted results, whereas the red-colored broken line represented actual results. Data are represented as mean ± SD.

immunohistochemical analyses of the matched samples were performed (Figure 3E). SLC17A9 showed high expression levels in cancer samples although it was also enriched in normal glomerular cells. These results further confirmed the upregulation of SLC17A9 in ccRCC.

High expression levels of SLC17A9 promote the proliferation of renal cancer cells

Although SLC17A9 was identified as a biomarker for renal cancer, its role in tumor growth was unknown. According to the latest study, SLC17A9 deficiency could lead to cell death via lysosome dysfunction-associated pathways,[7] indicating that SLC17A9 might influence the viability of renal cancer cells. As a result, the plasmid vector was transfected with SLC17A9 and siRNA to knock down SLC17A9 in 786-O and A498 cells. The mRNA levels of SLC17A9 were detected by qRT-PCR to validate the effects of siRNA and plasmid (Figures 4A–4D). WB experiments were performed to confirm the changes in the SLC17A9 protein levels after transfection (Figures 4E–4H). Next, cell counting kit-8 (CCK8) assays were carried out to demonstrate cell viability. As expected, the knockdown of SLC17A9 markedly inhibited the proliferation of two renal cancer cells (Figures 4I and 4J). The overexpression of SLC17A9 led to the upregulation of cell proliferation (Figures 4K–4L). These results indicated that SLC17A9 promoted the proliferation of ccRCC cells.

SLC17A9 contributed to the invasion and migration of renal cancer cells through the EMT signaling pathways

To determine the role of SLC17A9 in tumor progression, GSEA was conducted to investigate the potential biological processes using TCGA-KIRC data. The GSEA results revealed that SLC17A9 was positively

Table 1. Univariate and multivariate analyses of SLC17A9 expression and patient overall survival using TCGA-KIRC data (n = 522)

Variables	Univariate analysis			Multivariate analysis[c]		
	HR[a]	95%CI[b]	p value	HR[a]	95%CI[b]	p value
Age (years) ≤60 vs >60	1.753	1.290–2.383	<0.001	1.672	1.225–2.284	0.001
Gender Female vs Male	0.951	0.697–1.296	0.749	0.926	0.675–1.270	0.633
T stage T1 or T2 vs T3 or T4	3.159	2.331–4.281	<0.001	1.656	1.158–2.369	0.006
N stage N0 vs N1	3.883	2.102–7.174	<0.001	2.105	1.113–3.979	0.022
M stage M0 vs M1	4.358	3.194–5.946	<0.001	2.695	1.887–3.848	<0.001
Grade G1 or G2 vs G3 or G4	2.677	1.905–3.761	<0.001	1.573	1.079–2.292	0.018
SLC17A9 High vs Low	2.024	1.488–2.753	<0.001	1.507	1.089–2.086	0.013

[a]Hazard ratio, estimated from Cox proportional hazard regression model.

[b]Confidence interval of the estimated HR.

[c]Multivariate models were adjusted for T, N, M classification, age and gender.

Table 2. Univariate and multivariate analyses of SLC17A9 expression and patient disease free survival. using TCGA-KIRC data (n = 522)

Variables	Univariate analysis			Multivariate analysis[c]		
	HR[a]	95%CI[b]	p value	HR[a]	95%CI[b]	p value
Age (years) ≤60 vs >60	1.368	0.961–1.949	0.082	1.428	0.982–2.075	0.062
Gender Female vs Male	1.474	0.988–2.199	0.057	1.203	0.794–1.822	0.383
T stage T1 or T2 vs T3 or T4	4.441	3.080–6.405	<0.001	1.972	1.295–3.005	0.002
N stage N0 vs N1	5.837	2.928–11.635	<0.001	3.272	1.561–6.859	0.002
M stage M0 vs M1	8.413	5.789–12.226	<0.001	5.267	3.443–8.057	<0.001
Grade G1 or G2 vs G3 or G4	3.326	2.213–4.999	<0.001	2.151	1.394–3.320	0.001
SLC17A9 High vs Low	1.650	1.151–2.366	0.006	1.397	0.949–2.056	0.090

[a]Hazard ratio, estimated from Cox proportional hazard regression model.
[b]Confidence interval of the estimated HR.
[c]Multivariate models were adjusted for T, N, M classification, age and gender.

correlated with the cell cycle pathways and the G2M_checkpoint signaling (Figure 5A), thereby indicating that SLC17A9 could positively regulate cell proliferation as described in the previous section (Figures 4I–4L). It was also observed that SLC17A9 was significantly associated with the EMT process (Figure 5A), which was proven to contribute to the progression of almost all cancers. Furthermore, the effect of SLC17A9 on the EMT pathway in ccRCC was determined. The correlation analyses between SLC17A9 and four EMT markers (namely, CDH1, CDH2, SNAI1, and VIM) were conducted using TCGA-KIRC and ICGC-RECA-EU data (Figures 5B and S2C), thereby providing the initial evidence of the role of SLC17A9 in the EMT pathway in ccRCC. The results indicated that SLC17A9 was negatively correlated with CDH1 (r = −0.3401, p < 0.0001), and positively correlated with CDH2 (r = 0.1786, p < 0.0001), VIM (r = 0.3404, p < 0.0001), and SNAI1 (r = 0.2147, p < 0.0001) (Figure 5B). The results using ICGC-RECA-EU data are presented in Figure S2C. SLC17A9 knockdown led to the upregulation of E-cadherin and downregulation of N-cadherin, Snail, and Vimentin (Figures 5C and 5D). On the contrary, the overexpression of SLC17A9 could lead to the downregulation of E-cadherin and upregulation of N-cadherin, Snail, and Vimentin, indicating the promotion of the EMT pathway (Figures 5E and 5F). Finally, the invasion and migration experiments were conducted to validate the functional effects of the SLC17A9-EMT axis. SLC17A9 knockdown inhibited the invasion and migration of 786-O and A498 cells (Figures 5G and 5H). On the contrary, the overexpression of SLC17A9 significantly increased the invasion and migration of renal cancer cells (Figures 5I and 5J). These results demonstrated that SLC17A9 might affect ccRCC progression by promoting the EMT signaling pathways.

SLC17A9 promoted the proliferation and metastasis of RCC by PTHLH- dependent EMT process

The influence of the SLC17A9 mechanism on the EMT phenotype of ccRCC was investigated by analyzing the differentially expressed genes (DEGs) between the SLC17A9 high expression group and low expressions group based on the median expression levels of SLC17A9 from TCGA-KIRC data. Meanwhile, the EMT core gene set obtained from hallmark gene sets of GSEA software was used to screen the intersection genes, and four candidates (COL7A1, ADAM12, TGFBI, and PTHLH) were finally obtained (Figure 6A). The role of SLC17A9 in regulating the expression of the above genes was validated by qRT-PCR analyses after suppression or overexpression of SLC17A9 in 786-O and A498 cell lines. The results indicated that the overexpression of SLC17A9 could lead to the upregulation of PTHLH mRNA levels, and the suppression of SLC17A9 could lead to a decrease in the mRNA levels of PTHLH (Figures 6B and 6C). It was observed that the mRNA expression levels of COL7A1, ADAM12, and TGFBI were not regulated by SLC17A9.
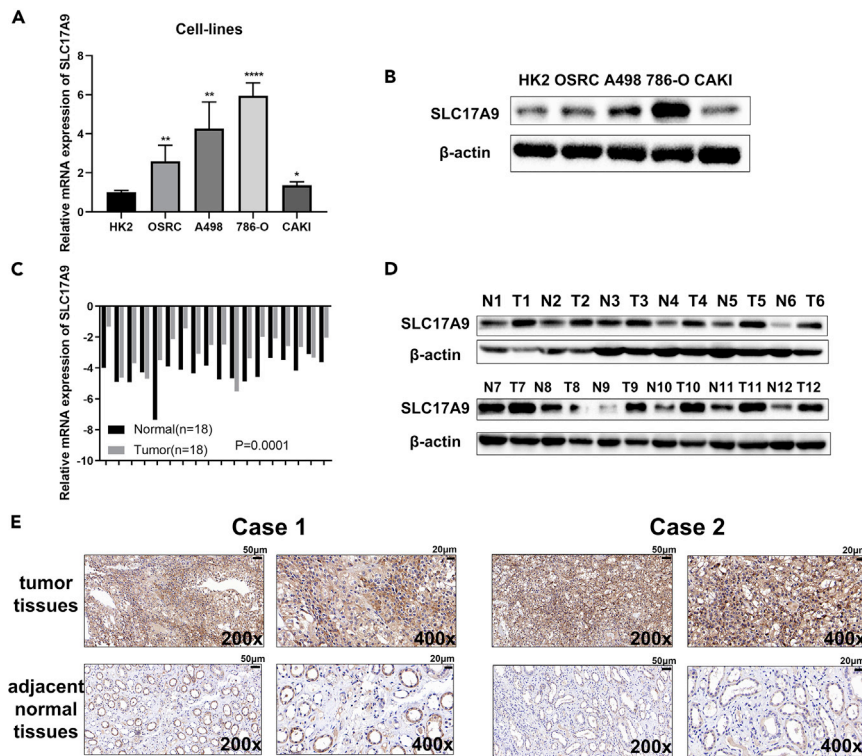
Figure 3. SLC17A9 was upregulated in ccRCC cell lines and tissues

(A and B) Relative mRNA and protein levels of SLC17A9 in ccRCC cell lines.

(C and D) Relative mRNA and protein levels of SLC17A9 in ccRCC tissues and adjacent normal kidney tissues.

(E) Immunohistochemistry (IHC) results (200x,400x) of SLC17A9 in ccRCC tissues and para-cancer tissues.

****$p < 0.0001$; ***$p < 0.001$; **$p < 0.01$; and *$p < 0.05$. Data are represented as mean $\pm$ SD. The length of scale bars are 50 and 20 μm.

Furthermore, WB experiments were performed and similar changes were observed by alteration of SLC17A9 (Figure 6D). Thus, PTHLH was identified as a downstream target of SLC17A9.

Although, PTHLH was reported to promote EMT in the renal tubular epithelial cells[18] and intestinal epithelial cells,[19] whether PTHLH could induce the EMT phenotype in ccRCC was still unknown. Firstly, PTHLH expression was knockdown and the changes in the EMT markers were analyzed (Figures S2D–S2G). The results revealed that the knockdown of PTHLH could decrease the expression of N-cadherin, Snail, and Vimentin, and increase the expression of E-cadherin, indicating that silent PTHLH could inhibit the EMT phenotype in ccRCC.

To further investigate the effect of SLC17A9 on EMT via PTHLH, WB and functional rescue experiments were conducted. The changes in the expression of EMT markers in SLC17A9-overexpressed renal cancer cells were evaluated by simultaneously knocking down PTHLH. The results indicated that PTHLH knockdown could decrease the expression of N-cadherin, Snail, and Vimentin, and increase the expression of E-cadherin, thereby effectively reversing the facilitation effect of SLC17A9 overexpression (Figures 6E and 6F). CCK-8 assays proved that the overexpression of SLC17A9 could contribute to the proliferation of 786-O and A498 cells while knocking down PTHLH could inhibit the promoting effect (Figure 6G). Functional rescue transwell experiments highlighted that silent PTHLH could partially decrease the migration and invasion of renal cancer cells in the high SLC17A9 expression group (Figure 6H). These findings indicated that the promotional effect of SLC17A9 on EMT in ccRCC was dependent on the activation of PTHLH.

High SLC17A9 expression might contribute to the immune therapy of ccRCC

Of interest, SLC17A9 was also found to be associated with interferon-gamma (INF-γ) and-alpha (INF-α) responses and IL6-JAK-STAT3 signaling pathways (Figure S2B). Because INF-α and-γ have been used for
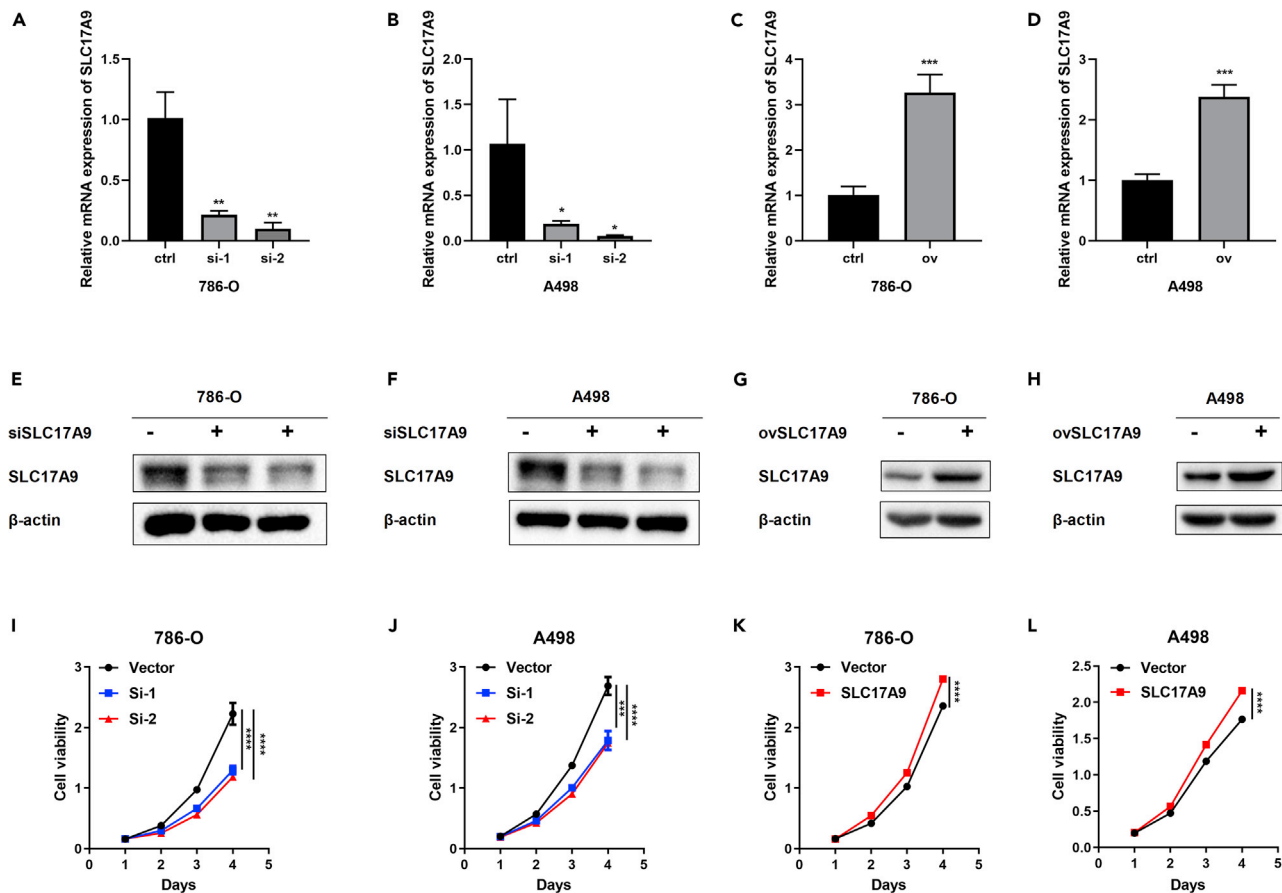
Figure 4. Effects of SLC17A9 on the proliferation of renal cancer cells

(A and B) Successful knockdown of SLC17A9 mRNA in 786-O and A498 cells.

(C and D) SLC17A9 mRNA levels were significantly overexpressed in 786-O and A498 cells.

(E and F) Protein levels after SLC17A9 knockdown in 786-O and A498 cells.

(G and H) Protein levels after SLC17A9 overexpression in 786-O and A498 cells.

(I–L) Cell counting kit-8 assays detected the effects of SLC17A9 overexpression and knockdown on the proliferation of 786-O and A498 cells. ****$p < 0.0001$; ***$p < 0.001$; **$p < 0.01$; and *$p < 0.05$. Data were presented as the mean ± standard deviation (SD) from three independent experiments.

anti-tumor therapy for a long time,[20–22] patients with higher SLC17A9 expression might show a better response to immunotherapy. SLC17A9-dependent ATP release has been reported to contribute to macrophage[23] and T cell[24] activation. Furthermore, the relationships between SLC17A9 and immune-associated features in ccRCC were investigated.

Comprehensive Analysis on Multi-Omics of Immunotherapy in Pan-cancer (CAMOIP) is an effective web-based tool that could help to analyze immune cells, genes, and scores of a single gene.[25] Firstly, the differences in the immune cell infiltration between the high SLC17A9 expression group and the low SLC17A9 level group were analyzed using TCGA-KIRC data (Figure S3A). The results indicated that the proportions of infiltration of plasma cells, CD8+T cells, Tfh cells, Tregs, and M0 macrophages in the high SLC17A9 group were significantly higher than those in low SLC17A9 groups. The infiltration levels of M1 macrophages and some other immune cells were lower in the high SLC17A9 group than those in the low SLC17A9 group. Furthermore, immune scores between the two groups were evaluated. As expected, patients with high SLC17A9 expression levels showed higher intratumor heterogeneity, proliferation, macrophage regulation, lymphocyte infiltration signature score, TGF-beta response, cancer-testis antigens (CTA) score, Th1 cells, and Th2 cells (Figure S3B). These results were consistent with our previous hypothesis that SLC17A9 showed a significant positive association with macrophage and T cell activation and cell cycle, and also indicated that SLC17A9 could lead to several immunosuppressive tumor microenvironments and play an important role in TGF-beta-associated treatments. Finally, the differences
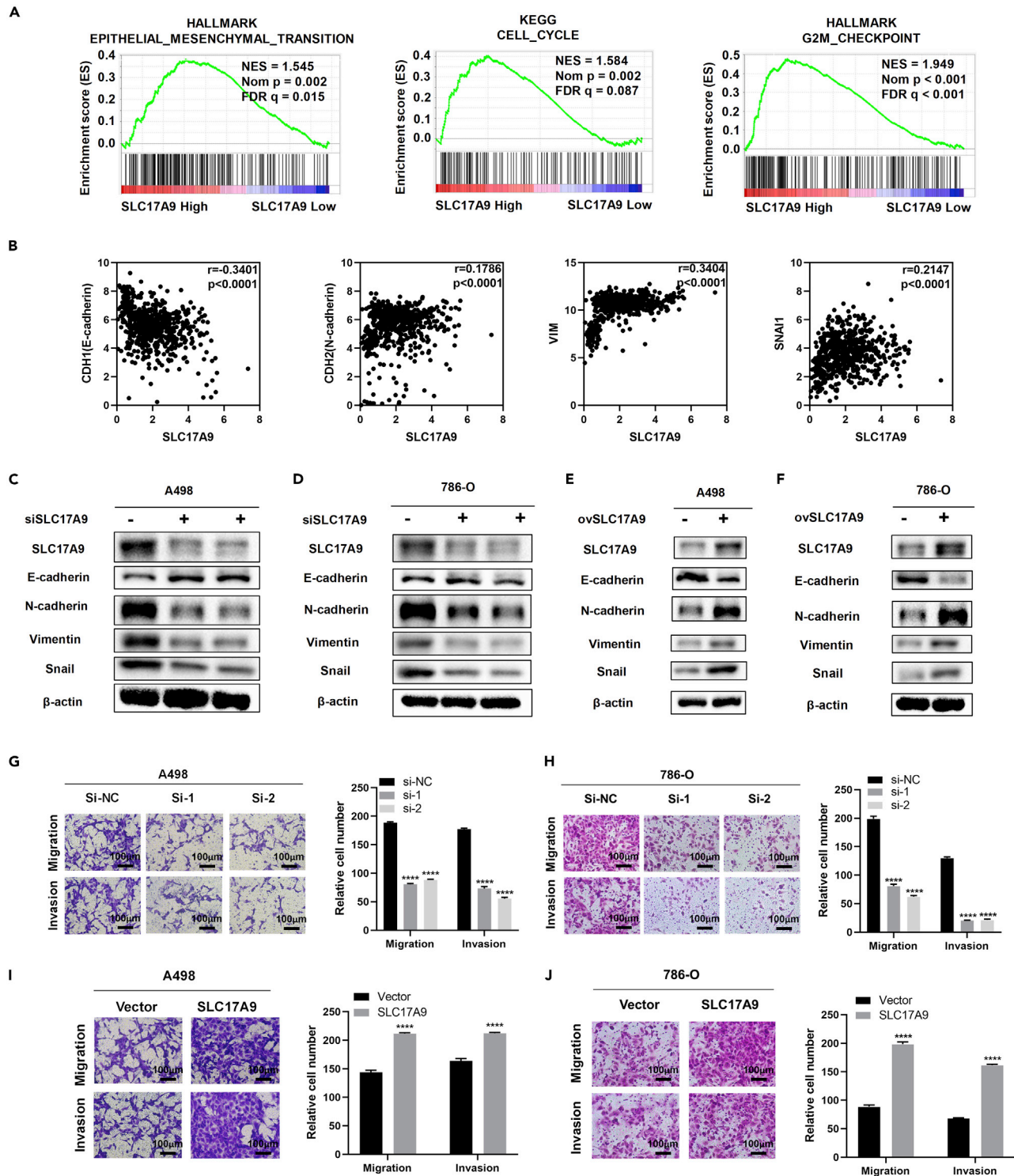
Figure 5. SLC17A9 affected renal cancer cells via EMT signaling pathways

(A) GSEA results of SLC17A9 using TCGA data.

(B) Correlation analyses of Snail, N-cadherin, E-cadherin, and vimentin with SLC17A9 were performed using the TCGA-KIRC data.

(C–F) Effects of SLC17A9 overexpression and knockdown on E-cadherin, N-cadherin, vimentin, and snail-1 in renal cancer cells.

(G–J) Effects of SLC17A9 overexpression and knockdown on cell migration and invasion. ****p < 0.0001. Data are represented as mean ± SD. The length of scale bar is 100 μm.
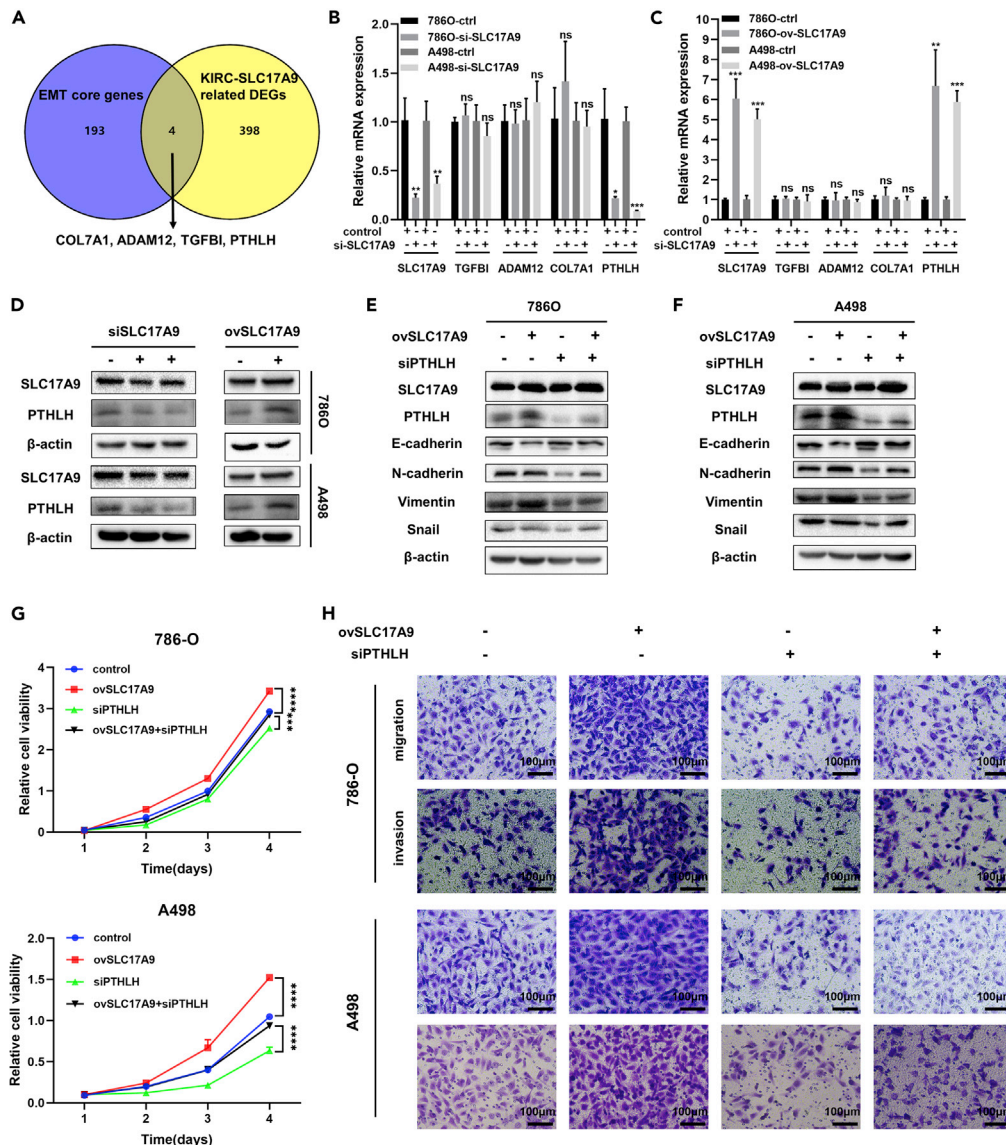
Figure 6. SLC17A9-activated EMT pathway was dependent on PTHLH

(A) Four potential downstream genes of SLC17A9.

(B and C) Regulation of PTHLH by SLC17A9 was verified at the mRNA level.

(D) Regulation of PTHLH by SLC17A9 was verified at the protein level.

(E and F) Knockdown of PTHLH could reverse the effect of SLC17A9 overexpression on EMT markers.

(G and H) Migration and invasion assays (200x) for the indicated ccRCC cells. ****$p < 0.0001$; ***$p < 0.001$; **$p < 0.01$; and *$p < 0.05$. Data are represented as mean $\pm$ SD. The length of scale bar is 100 μm.

in the expression of some common immune checkpoints between the two groups were analyzed. It was observed that the expression of almost all the immune checkpoints was much higher in the SLC17A9 high expression group, indicating that SLC17A9 might promote the malignant development of ccRCC by influencing immunosuppressive microenvironments, and inhibition of SLC17A9 could help in ccRCC treatment (Figures S3C–S3D).

SLC17A9 might be a target for several drugs and also related to drug resistance

Because SLC17A9 is an important membrane transport protein and is considered to significantly participate in the progression of several cancers, it is necessary to investigate potential drugs targeting SLC17A9. CellMiner is an open database that integrates data on the response of human cancer cell
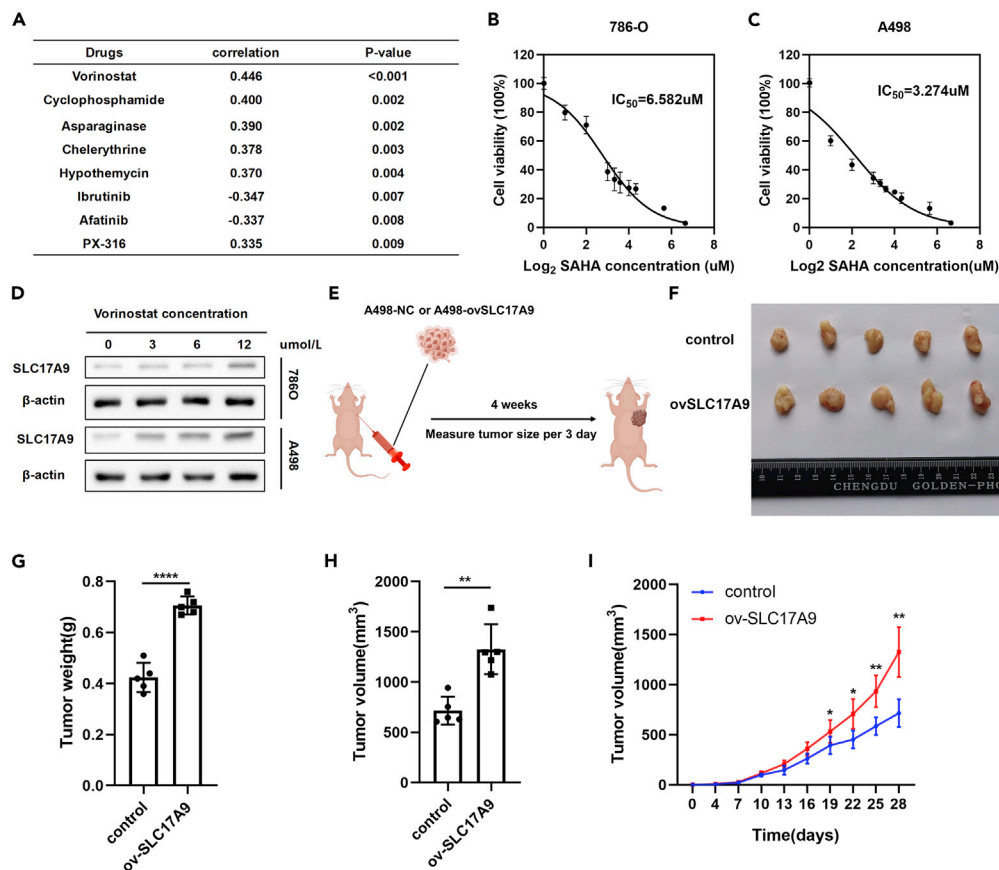
Figure 7. Upregulation of SLC17A9 promoted tumor progression *in vivo*

(A) Prediction of SLC17A9 associated drugs.

(B and C) IC_{50} of vorinostat in A498 and 786-O.

(D) Protein expression levels of SLC17A9 in cells cultivated at different vorinostat concentrations.

(E–I) Subcutaneous tumor in mice, its growth curve, and final volume and weight (n = 5).

****$p < 0.0001$; ***$p < 0.001$; **$p < 0.01$; and *$p < 0.05$. Data are represented as mean $\pm$ SD.

lines to multiple drugs.[26] CellMiner was used to assess the correlation between SLC17A9 and drugs approved by Food and Drug Administration (FDA) for clinical therapy (Figure 7A). The results highlighted that the half maximal inhibitory concentrations (IC_{50}) of vorinostat, cyclophosphamide, asparaginase, chelerythrine, hypothemycin, and PX-316 (an AKT inhibitor) were positively associated with SLC17A9 expression levels (Figures S4A–S4E and S4H), indicating that high SLC17A9 expression might contribute to resistance to drugs mentioned above. IC_{50} of ibrutinib and afatinib were negatively related to SLC17A9 expression (Figures S4F–S4G), indicating SLC17A9 might play a role in their anti-tumor effect. The patients with higher SLC17A9 expression could be sensitive to ibrutinib and afatinib.

Vorinostat (also called SAHA) was found to be the most relative drug associated with SLC17A9, and multiple clinical trials have been conducted to elucidate its effectiveness for the treatment of RCC. Therefore, this study also examined the preliminary relationship of vorinostat with SLC17A9 *in vitro*. First, the IC_{50} values of vorinostat in 786-O and A498 cells were evaluated, and the results indicated that the IC_{50} of vorinostat for 786-O cells was 6.582 μM and for A498 was 3.274 uM (Figures 7B and 7C). Second, the renal cancer cells were cultured for 48 h in the medium containing vorinostat at the fold increase in IC_{50} concentration and were used for subsequent WB experiments. It was observed that the protein expression of SLC17A9 increased with an increase in vorinostat concentrations (Figure 7D). This indicated that SLC17A9 might play a role in inducting vorinostat resistance in ccRCC, although more studies are needed to confirm this.

SLC17A9 played a significant role in the progression of ccRCC *in vivo*

Although it was confirmed that SLC17A9 played a significant role in ccRCC progression *in vitro*, further validation *in vivo* was necessary. A498 cells stably transfected with overexpressing SLC17A9 virus or control virus were injected into Balb/c nude mice. The size of the tumors was measured every third day, and the fully grown tumors were obtained on the 28th day (Figure 7E). The results *in vivo* confirmed that tumor weights and volumes in the SLC17A9 overexpression group were significantly higher than those in the control group (Figures 7F–7I), indicating that SLC17A9 was significant for the growth and progression of ccRCC.

DISCUSSION

Although it was reported that SLC17A9 acted as an oncogene for prostate cancer,[9] hepatocellular carcinoma,[12] gastric carcinoma,[11] and colorectal cancer,[10] the role of SLC17A9 in ccRCC has not been studied. TCGA-KIRC data was used to evaluate the expression levels of SLC17A9 in renal cancer, and ICGC-RECA-EU data was used to validate its high expression. The expression of SLC17A9 increased with the increase in the tumor stage and grade, indicating that SLC17A9 could act as an indicator of increased malignancy. Furthermore, certain diagnostic value of SLC17A9 was identified using ROC curves, and prognostic value was identified using KM survival analyses and cox regression analyses. An effective nomogram model was also constructed to predict individual survival time, which highlighted that SLC17A9 could be a potential biomarker in ccRCC.

Furthermore, a series of experiments were conducted to validate the expression of SLC17A9 and evaluate its function and mechanism. WB, qRT-PCR, and immunohistochemistry results indicated that SLC17A9 was truly upregulated in ccRCC. SLC17A9 knockdown inhibited the proliferation, invasion, and migration of A498 and 786-O cells, whereas overexpression of SLC17A9 reversed this phenomenon. Furthermore, GSEA was conducted to determine the potential mechanisms by which SLC17A9 influences ccRCC. SLC17A9 showed a significant positive association with EMT, cell cycle, G2M_checkpoint, and E2F_targets, which was in agreement with the previous results. The upregulation of SLC17A9 led to the downregulation of E-cadherin and upregulation of N-cadherin, snail, and vimentin, thereby contributing to EMT. Moreover, it was also observed that common cancer-promoting signaling pathways, including myc targets and hedgehog-signaling pathways, were associated with SLC17A9.[27,28]

The mechanism involved in the promotion of EMT by SLC17A9 was further elucidated by applying the TCGA data and EMT core gene sets to determine PTHLH, which might be the potential EMT-associated SLC17A9 target gene. It was proven that PTHLH positively regulated EMT in renal tubular epithelial cells and intestinal epithelial cells, and is regarded as one of the EMT regulators, thus elucidating the role of PTHLH in promoting EMT in ccRCC. PTHLH knockdown led to a decrease in N-cadherin, Snail, and Vimentin and an increase in E-cadherin. By monitoring the changes in the EMT markers in both SLC17A9-overexpressing and PTHLH-silencing 786-O or A498 cells, it was observed that the EMT-promoting effect of SLC17A9 could be blocked by silencing PTHLH. This was also in agreement with the results observed in the functional experiments. Thus, these results proved that the promotion of EMT by SLC17A9 was dependent on PTHLH.

SLC17A9 has been previously reported to affect T-cell and macrophage activation,[23,24] thereby highlighting its immune function. Moreover, as SLC17A9 was important for ATP production, and several studies have revealed that ATP-associated genes,[29,30] such as CD39, could significantly influence tumor immunity and therapy, it is important to determine the role of SLC17A9 in immune infiltration and therapy in ccRCC. Regulatory T cells (Tregs) were generally reported to promote tumor progression,[31] whereas M1 macrophages were believed to possess anti-tumor activity.[32,33] It can be stated that SLC17A9 might increase Tregs infiltration or reduce M1 polarization to promote ccRCC development; however, further research is required to provide evidence. Intratumor heterogeneity,[34] proliferation, and CTA[35] were reported to be closely related to the increase in tumor malignancy. The results from this study indicated that high expression of SLC17A9 might promote malignancy of ccRCC by the factors discussed above. Moreover, patients with high SLC17A9 levels showed higher macrophage regulation scores, lymphocyte infiltration signature scores, TGF-beta response scores, Th1 cell scores, and Th2 cell scores, thereby highlighting the complex effects of SLC17A9 on the immune microenvironment. Immune checkpoint inhibitors have been extensively studied and applied to the clinical treatment of several cancers.[36–38] This study observed that 12 common immune checkpoint molecules,[39] represented by PD1, CTLA4, and LAG3, were highly

expressed in the SLC17A9 high-expression group. Thus, the inhibition of SLC17A9 might help to improve the suppressive microenvironment of ccRCC by interfering with these molecules.

SLC17A9 is an important ATP transport protein and is correlated with several drugs. It was reported that clodronate could help in the therapy of steatohepatitis and acute liver injury by inhibiting SLC17A9.[13] Streptozotocin induced diabetic bladder dysfunction by upregulating SLC17A9.[40] CellMiner database was used to determine SLC17A9-associated potential drugs, and the results are shown in Figure S4. Notably, most of the eight drugs had been evaluated for the treatment of renal cancer and some of them even completed clinical trials.[41–43] For example, histone deacetylase inhibitor vorinostat has been used in combination with multiple other drugs for the treatment of kidney cancer.[44–46] The study results revealed that SLC17A9 might be associated with resistance to vorinostat and the other five drugs as discussed previously. SLC17A9 might play multiple roles in the treatment of tumors with ibrutinib and afatinib. To further validate this hypothesis, the most relative drug vorinostat was selected to perform subsequent experiments. The study results highlighted that the protein levels of SLC17A9 increased with the increase in vorinostat concentration, indicating that SLC17A9 might play a role in vorinostat resistance in ccRCC. However, this hypothesis needs more rigorous validation in the future.

Finally, the effect of SLC17A9 in ccRCC *in vivo* was validated by the tumor implantation experiment. The results indicated that overexpression of SLC17A9 could contribute to tumor growth and progression.

In this study, SLC17A9 served as an unfavorable diagnostic and prognostic biomarker for ccRCC, and the results indicated that SLC17A9 promoted the progression of ccRCC via the PTHLH-induced EMT process. SLC17A9 might interfere with multiple immunological processes to affect the progression of ccRCC. Finally, based on the results, the potential therapeutic drugs were predicted in this study.

Limitations of the study

This study has some limitations, which should be overcome in future studies. GSEA indicated that SLC17A9 might influence several pathways; however, all of these pathways were not investigated in detail. In this study, it was believed that high expression of SLC17A9 might be helpful for immune therapy. However, this hypothesis needs further validation. Several drugs had been analyzed by the open-resource data, but some of them were not verified in this study. Although the relationship between SLC17A9 expression and vorinostat concentration was initially determined, the mechanism was not elucidated in this study. It is important to study the multiple roles of SLC17A9 as an oncogene in ccRCC considering all these aspects in the future.

ETHICS APPROVAL AND CONSENT TO PARTICIPATE

All the procedures performed in studies involving human participants were in accordance with the ethical standards of the Institutional Review Board of Huazhong University of Science and Technology (S175).

CONSENT FOR PUBLICATION

All the authors consent to the publication of this manuscript.

STAR★METHODS

Detailed methods are provided in the online version of this paper and include the following:

- KEY RESOURCES TABLE
- RESOURCE AVAILABILITY
  - Lead contact
  - Materials availability
  - Data and code availability
- EXPERIMENTAL MODEL AND SUBJECT DETAILS
  - Animal experiments *in vivo*
  - Cell culture and transient transfection of SLC17A9
- METHOD DETAILS
  - Clinical tissues collection
  - RNA extraction and qRT-PCR experiments

- ○ Cell proliferation array
- ○ Migratory and invasion assays
- ○ Immunohistochemistry (IHC) arrays
- ○ Western blotting (WB)
- ○ Bioinformatics analysis
- ● QUANTIFICATION AND STATISTICAL ANALYSES

SUPPLEMENTAL INFORMATION

Supplemental information can be found online at https://doi.org/10.1016/j.isci.2022.105764.

AUTHOR CONTRIBUTIONS

W.Q.L., X.N., and X.G.M. performed experiments, performed data analyses, and drafted the manuscript. W.Q.L., X.N., and X.G.M. contributed equally to this study. H.W.Y., T.X.Y., Q.M., and H.M.Y. contributed to reviewing the manuscript. B.H., W.X., and X.P.Z. designed and supervised the study. All the authors read and approved the final manuscript.

DECLARATION OF INTERESTS

The authors declare that they have no competing interests.

REFERENCES

1. Siegel, R.L., Miller, K.D., Fuchs, H.E., and Jemal, A. (2022). Cancer statistics, 2022. CA. Cancer J. Clin. *72*, 7–33.

2. Kang, M.J., Won, Y.J., Lee, J.J., Jung, K.W., Kim, H.J., Kong, H.J., Im, J.S., and Seo, H.G.; Community of Population-Based Regional Cancer Registries (2022). Cancer statistics in Korea: incidence, mortality, survival, and prevalence in 2019. Cancer Res. Treat. *54*, 330–344.

3. Xia, C., Dong, X., Li, H., Cao, M., Sun, D., He, S., Yang, F., Yan, X., Zhang, S., Li, N., and Chen, W. (2022). Cancer statistics in China and United States, 2022: profiles, trends, and determinants. Chin. Med. J. *135*, 584–590.

4. Global Burden of Disease 2019 Cancer Collaboration, Kocarnik, J.M., Compton, K., Dean, F.E., Fu, W., Gaw, B.L., Harvey, J.D., Henrikson, H.J., Lu, D., Pennini, A., Xu, R., et al. (2022). Cancer incidence, mortality, years of life lost, years lived with disability, and disability-adjusted life years for 29 cancer groups from 2010 to 2019: a systematic analysis for the global burden of disease study 2019. JAMA Oncol. *8*, 420–444.

5. Capitanio, U., Bensalah, K., Bex, A., Boorjian, S.A., Bray, F., Coleman, J., Gore, J.L., Sun, M., Wood, C., and Russo, P. (2019). Epidemiology of renal cell carcinoma. Eur. Urol. *75*, 74–84.

6. Moch, H., Cubilla, A.L., Humphrey, P.A., Reuter, V.E., and Ulbright, T.M. (2016). The 2016 WHO classification of tumours of the urinary system and male genital organs-Part A: renal, penile, and testicular tumours. Eur. Urol. *70*, 93–105.

7. Huang, P., Cao, Q., Xu, M., and Dong, X.P. (2022). Lysosomal ATP transporter SLC17A9 controls cell viability via regulating cathepsin D. Cells *11*, 887.

8. Cao, Q., Zhao, K., Zhong, X.Z., Zou, Y., Yu, H., Huang, P., Xu, T.L., and Dong, X.P. (2014). SLC17A9 protein functions as a lysosomal ATP transporter and regulates cell viability. J. Biol. Chem. *289*, 23189–23199.

9. Mi, Y.Y., Sun, C.Y., Zhang, L.F., Wang, J., Shao, H.B., Qin, F., Xia, G.W., and Zhu, L.J. (2021). Long non-coding RNAs LINC01679 as a competitive endogenous RNAs inhibits the development and progression of prostate cancer via regulating the miR-3150a-3p/SLC17A9 Axis. Front. Cell Dev. Biol. *9*, 737812.

10. Yang, L., Chen, Z., Xiong, W., Ren, H., Zhai, E., Xu, K., Yang, H., Zhang, Z., Ding, L., He, Y., et al. (2019). High expression of SLC17A9 correlates with poor prognosis in colorectal cancer. Hum. Pathol. *84*, 62–70.

11. Sun, M., Qiu, J., Zhai, H., Wang, Y., Ma, P., Li, M., and Chen, B. (2020). Prognostic implications of novel gene signatures in gastric cancer microenvironment. Med. Sci. Monit. *26*, e924604.

12. Wu, J., Yang, Y., and Song, J. (2020). Expression of SLC17A9 in hepatocellular carcinoma and its clinical significance. Oncol. Lett. *20*, 182.

13. Hasuzawa, N., Tatsushima, K., Wang, L., Kabashima, M., Tokubuchi, R., Nagayama, A., Ashida, K., Ogawa, Y., Moriyama, Y., and Nomura, M. (2021). Clodronate, an inhibitor of the vesicular nucleotide transporter, ameliorates steatohepatitis and acute liver injury. Sci. Rep. *11*, 5192.

14. Hasuzawa, N., Tatsushima, K., Tokubuchi, R., Kabashima, M., and Nomura, M. (2021). [VNUT is a therapeutic target for type 2 diabetes and NASH]. Yakugaku Zasshi *141*, 517–526.

15. Kinoshita, M., Hirayama, Y., Fujishita, K., Shibata, K., Shinozaki, Y., Shigetomi, E., Takeda, A., Le, H.P.N., Hayashi, H., Hiasa, M., et al. (2018). Anti-depressant fluoxetine reveals its therapeutic effect via astrocytes. EBioMedicine *32*, 72–83.

16. Hanahan, D. (2022). Hallmarks of cancer: new dimensions. Cancer Discov. *12*, 31–46.

17. Brabletz, T., Kalluri, R., Nieto, M.A., and Weinberg, R.A. (2018). EMT in cancer. Nat. Rev. Cancer *18*, 128–134.

18. Ardura, J.A., Rayego-Mateos, S., Rámila, D., Ruiz-Ortega, M., and Esbrit, P. (2010). Parathyroid hormone-related protein promotes epithelial-mesenchymal transition. J. Am. Soc. Nephrol. *21*, 237–248.

19. He, S., Xue, M., Liu, C., Xie, F., and Bai, L. (2018). Parathyroid hormone-like hormone induces epithelial-to-mesenchymal transition of intestinal epithelial cells by activating the runt-related transcription factor 2. Am. J. Pathol. *188*, 1374–1388.

20. Larson, R.C., Kann, M.C., Bailey, S.R., Haradhvala, N.J., Llopis, P.M., Bouffard, A.A., Scarfó, I., Leick, M.B., Grauwet, K., Berger, T.R., et al. (2022). CAR T cell killing requires the IFNγR pathway in solid but not liquid tumours. Nature *604*, 563–570.

21. Hu, B., Yu, M., Ma, X., Sun, J., Liu, C., Wang, C., Wu, S., Fu, P., Yang, Z., He, Y., et al. (2022). Interferon-a potentiates anti-PD-1 efficacy by remodeling glucose metabolism in the hepatocellular carcinoma microenvironment. Cancer Discov. *12*, 1718–1741.

22. Ravaud, A., Barrios, C.H., Alekseev, B., Tay, M.H., Agarwala, S.S., Yalcin, S., Lin, C.C., Roman, L., Shkolnik, M., Anak, O., et al. (2015). RECORD-2: phase II randomized study of everolimus and bevacizumab versus interferon α-2a and bevacizumab as first-line therapy in patients with metastatic renal cell carcinoma. Ann. Oncol. *26*, 1378–1384.

23. Sakaki, H., Tsukimoto, M., Harada, H., Moriyama, Y., and Kojima, S. (2013). Autocrine regulation of macrophage activation via exocytosis of ATP and activation of P2Y11 receptor. PLoS One *8*, e59778.

24. Tokunaga, A., Tsukimoto, M., Harada, H., Moriyama, Y., and Kojima, S. (2010). Involvement of SLC17A9-dependent vesicular exocytosis in the mechanism of ATP release during T cell activation. J. Biol. Chem. *285*, 17406–17416.

25. Lin, A., Qi, C., Wei, T., Li, M., Cheng, Q., Liu, Z., Luo, P., and Zhang, J. (2022). CAMOIP: a web server for comprehensive analysis on multi-omics of immunotherapy in pan-cancer. Brief. Bioinform. *23*, bbac129.

26. Reinhold, W.C., Sunshine, M., Liu, H., Varma, S., Kohn, K.W., Morris, J., Doroshow, J., and Pommier, Y. (2012). CellMiner: a web-based suite of genomic and pharmacologic tools to explore transcript and drug patterns in the NCI-60 cell line set. Cancer Res. *72*, 3499–3511.

27. Grampp, S., Platt, J.L., Lauer, V., Salama, R., Kranz, F., Neumann, V.K., Wach, S., Stöhr, C., Hartmann, A., Eckardt, K.U., et al. (2016). Genetic variation at the 8q24.21 renal cancer susceptibility locus affects HIF binding to a MYC enhancer. Nat. Commun. *7*, 13183.

28. Li, G., Ci, W., Karmakar, S., Chen, K., Dhar, R., Fan, Z., Guo, Z., Zhang, J., Ke, Y., Wang, L., et al. (2014). SPOP promotes tumorigenesis by acting as a key regulatory hub in kidney cancer. Cancer Cell *25*, 455–468.

29. Moesta, A.K., Li, X.Y., and Smyth, M.J. (2020). Targeting CD39 in cancer. Nat. Rev. Immunol. *20*, 739–755.

30. Li, X.Y., Moesta, A.K., Xiao, C., Nakamura, K., Casey, M., Zhang, H., Madore, J., Lepletier, A., Aguilera, A.R., Sundarrajan, A., et al. (2019). Targeting CD39 in cancer reveals an extracellular ATP- and inflammasome-driven tumor immunity. Cancer Discov. *9*, 1754–1773.

31. Huppert, L.A., Green, M.D., Kim, L., Chow, C., Leyfman, Y., Daud, A.I., and Lee, J.C. (2022). Tissue-specific Tregs in cancer metastasis: opportunities for precision immunotherapy. Cell. Mol. Immunol. *19*, 33–45.

32. Kuo, W.T., Chang, J.M., Chen, C.C., Tsao, N., and Chang, C.P. (2022). Autophagy drives plasticity and functional polarization of tumor-associated macrophages. IUBMB Life *74*, 157–169.

33. Mantovani, A., Marchesi, F., Malesci, A., Laghi, L., and Allavena, P. (2017). Tumour-associated macrophages as treatment targets in oncology. Nat. Rev. Clin. Oncol. *14*, 399–416.

34. Milo, I., Bedora-Faure, M., Garcia, Z., Thibaut, R., Périé, L., Shakhar, G., Deriano, L., and Bousso, P. (2018). The immune system profoundly restricts intratumor genetic heterogeneity. Sci. Immunol. *3*, eaat1435.

35. Maxfield, K.E., Taus, P.J., Corcoran, K., Wooten, J., Macion, J., Zhou, Y., Borromeo, M., Kollipara, R.K., Yan, J., Xie, Y., et al. (2015). Comprehensive functional characterization of cancer-testis antigens defines obligate participation in multiple hallmarks of cancer. Nat. Commun. *6*, 8840.

36. Choueiri, T.K., Motzer, R.J., Rini, B.I., Haanen, J., Campbell, M.T., Venugopal, B., Kollmannsberger, C., Gravis-Mescam, G., Uemura, M., Lee, J.L., et al. (2020). Updated efficacy results from the JAVELIN Renal 101 trial: first-line avelumab plus axitinib versus sunitinib in patients with advanced renal cell carcinoma. Ann. Oncol. *31*, 1030–1039.

37. Kartolo, A., Kassouf, W., and Vera-Badillo, F.E. (2021). Adjuvant immune checkpoint inhibition in muscle-invasive bladder cancer: is it ready for prime time? Eur. Urol. *80*, 679–681.

38. Regan, M.M., Werner, L., Rao, S., Gupte-Singh, K., Hodi, F.S., Kirkwood, J.M., Kluger, H.M., Larkin, J., Postow, M.A., Ritchings, C., et al. (2019). Treatment-free survival: a novel outcome measure of the effects of immune checkpoint inhibition-A pooled analysis of patients with advanced melanoma. J. Clin. Oncol. *37*, 3350–3358.

39. Topalian, S.L., Taube, J.M., Anders, R.A., and Pardoll, D.M. (2016). Mechanism-driven biomarkers to guide immune checkpoint blockade in cancer therapy. Nat. Rev. Cancer *16*, 275–287.

40. Yang, X.F., Wang, J., Rui, W., Xu, Y.F., Chen, F.J., Tang, L.Y., Ren, W.K., Fu, L.J., Tan, B., Huang, P., and Cao, H.Y. (2019). Time-dependent functional, morphological, and molecular changes in diabetic bladder dysfunction in streptozotocin-induced diabetic mice. Neurourol. Urodyn. *38*, 1266–1277.

41. Huijts, C.M., Lougheed, S.M., Bodalal, Z., van Herpen, C.M., Hamberg, P., Tascilar, M., Haanen, J.B., Verheul, H.M., de Gruijl, T.D., and van der Vliet, H.J.; Dutch WIN-O Consortium (2019). The effect of everolimus and low-dose cyclophosphamide on immune cell subsets in patients with metastatic renal cell carcinoma: results from a phase I clinical trial. Cancer Immunol. Immunother. *68*, 503–515.

42. He, H., Zhuo, R., Dai, J., Wang, X., Huang, X., Wang, H., and Xu, D. (2020). Chelerythrine induces apoptosis via ROS-mediated endoplasmic reticulum stress and STAT3 pathways in human renal cell carcinoma. J. Cell Mol. Med. *24*, 50–60.

43. Meuillet, E.J., Ihle, N., Baker, A.F., Gard, J.M., Stamper, C., Williams, R., Coon, A., Mahadevan, D., George, B.L., Kirkpatrick, L., and Powis, G. (2004). In vivo molecular pharmacology and antitumor activity of the targeted Akt inhibitor PX-316. Oncol. Res. *14*, 513–527.

44. Molina, A.M., van der Mijn, J.C., Christos, P., Wright, J., Thomas, C., Dutcher, J.P., Nanus, D.M., Tagawa, S.T., and Gudas, L.J. (2020). NCI 6896: a phase I trial of vorinostat (SAHA) and isotretinoin (13-cis retinoic acid) in the treatment of patients with advanced renal cell carcinoma. Invest. New Drugs *38*, 1383–1389.

45. Pili, R., Liu, G., Chintala, S., Verheul, H., Rehman, S., Attwood, K., Lodge, M.A., Wahl, R., Martin, J.I., Miles, K.M., et al. (2017). Combination of the histone deacetylase inhibitor vorinostat with bevacizumab in patients with clear-cell renal cell carcinoma: a multicentre, single-arm phase I/II clinical trial. Br. J. Cancer *116*, 874–883.

46. Zibelman, M., Wong, Y.N., Devarajan, K., Malizzia, L., Corrigan, A., Olszanski, A.J., Denlinger, C.S., Roethke, S.K., Tetzlaff, C.H., and Plimack, E.R. (2015). Phase I study of the mTOR inhibitor ridaforolimus and the HDAC inhibitor vorinostat in advanced renal cell carcinoma and other solid tumors. Invest. New Drugs *33*, 1040–1047.

47. Meng, X., Xiong, Z., Xiao, W., Yuan, C., Wang, C., Huang, Y., Tong, J., Shi, J., Chen, Z., Liu, C., et al. (2020). Downregulation of ubiquitin-specific protease 2 possesses prognostic and diagnostic value and promotes the clear cell

renal cell carcinoma progression. Ann. Transl. Med. *8*, 319.

48. Meng, X., Li, W., Yuan, H., Dong, W., Xiao, W., and Zhang, X. (2022). KDELR2-KIF20A axis facilitates bladder cancer growth and metastasis by enhancing Golgi-mediated secretion. Biol. Proced. Online *24*, 12.

49. Xiao, W., Xiong, Z., Xiong, W., Yuan, C., Xiao, H., Ruan, H., Song, Z., Wang, C., Bao, L., Cao, Q., et al. (2019). Melatonin/PGC1A/UCP1 promotes tumor slimming and represses tumor progression by initiating autophagy and lipid browning. J. Pineal Res. *67*, e12607.

50. Li, W., Meng, X., Yuan, H., Xiao, W., and Zhang, X. (2022). M2-polarization-related CNTNAP1 gene might be a novel immunotherapeutic target and biomarker for clear cell renal cell carcinoma. IUBMB Life *74*, 391–407.

51. Xiao, W., Wang, C., Chen, K., Wang, T., Xing, J., Zhang, X., and Wang, X. (2020). MiR-765 functions as a tumour suppressor and eliminates lipids in clear cell renal cell carcinoma by downregulating PLP2. EBioMedicine *51*, 102622.

52. Reinhold, W.C., Sunshine, M., Varma, S., Doroshow, J.H., and Pommier, Y. (2015). Using CellMiner 1.6 for systems pharmacology and genomic analysis of the NCI-60. Clin. Cancer Res. *21*, 3841–3852.

STAR★METHODS

KEY RESOURCES TABLE

REAGENT or RESOURCE	SOURCE	IDENTIFIER
Antibodies		
SLC17A9	Proteintech	Cat# 26731-1-AP; RRID:AB_2880617
Snail	ABclonal	Cat# A5243; RRID:AB_2766076
E-cadherin	ABclonal	Cat# A11509; RRID:AB_2758587
vimentin	ABclonal	Cat# A11952; RRID:AB_2861643
β-actin	ABclonal	Cat# AC026; RRID:AB_2768234
PTHLH	ABclonal	Cat# A3183; RRID:AB_2764970
Chemicals, peptides, and recombinant proteins		
Vorinostat/SAHA	BIOSEN	BES2310
Critical commercial assays		
CCK8	MedChemExpress	HY-K0301
Experimental models: Cell lines		
HK2	ATCC	CRL-2190
OSRC-2	NICR	1101HUM-PUMC000292
786-O	ATCC	CRL-1932
A498	ATCC	HTB-44
CAKI-1	ATCC	HTB-46
Experimental models: Organisms/strains		
BALB/c	Beijing Vital River Laboratory Animal Technology Co., Ltd	N/A
Oligonucleotides		
GAPDH-Forward:5′-GAGTCAACGGATTTGGTCGT-3′	Sangon Biotech	N/A
GAPDH-Reverse:5′-GACAAGCTTCCCGTTCTCAG-3′	Sangon Biotech	N/A
SLC17A9 Forward:5′- CACCTCGGGGATCGGATTG-3′	Sangon Biotech	N/A
SLC17A9 Reverse:5′-GCAGGGAAGTAAACCCCTTGG-3′	Sangon Biotech	N/A
COL7A1 Forward:5′-AAGGACCTCGGGGGAGACAAT-3′	Sangon Biotech	N/A
COL7A1 Reverse:5′-CGGATACCAGGCACTCCATC-3′	Sangon Biotech	N/A
ADAM12 Forward:5′-CCCATCCGGCAAGCAGATAA-3′	Sangon Biotech	N/A
ADAM12 Reverse:5′-CACAAATCCGGCAGCAAGAA-3′	Sangon Biotech	N/A
TGFBI Forward:5′-AGGCCTTCGAGAAGATCCCT-3′	Sangon Biotech	N/A
TGFBI Reverse:5′-CAACGATGGCTTCAGCACAC-3′	Sangon Biotech	N/A
PTHLH Forward:5′-CCGTCCGATTTGGGTCTGAT-3′	Sangon Biotech	N/A
PTHLH Reverse:5′-GAGTCTAACCAGGCAGAGCG-3′	Sangon Biotech	N/A
siPTHLH-1:5′-GAAGUCCAUCCAAGAUUUAUT-3′	GenePharma	N/A
siPTHLH-2:5′-GAUGAGGGCAGAUACCUAAT-3′	GenePharma	N/A
siSLC17A9-1: 5′-GCUGGCAGAGCAUCUUCUATT-3′	GenePharma	N/A
siSLC17A9-2: 5′-CCAAGGGCUGGAUCUUCAATT-3′	GenePharma	N/A
Recombinant DNA		
SLC17A9-plasmid	GeneChem	N/A
Software and algorithms		
GraphPad Prism 8.0	GraphPad Prism Software, Inc	

Continued		
REAGENT or RESOURCE	SOURCE	IDENTIFIER
SPSS Statistics 23.0	IBM Corporation, Armonk NY, USA	
R-4.0.3	R	

RESOURCE AVAILABILITY

Lead contact

Further information and requests for resources and reagents should be directed to and will be fulfilled by the Lead Contact, Xiaoping Zhang at xzhang@hust.edu.cn.

Materials availability

This study did not generate new unique reagents and all materials in this study are commercially available.

Data and code availability

Data: All the data reported in this study will be shared by the lead contact upon request.

Code: This study does not report any original code.

Additional information: Any additional information required to reanalyze the data reported in this study is available from the lead contact upon reasonable request.

EXPERIMENTAL MODEL AND SUBJECT DETAILS

Animal experiments *in vivo*

BALB/c nude mice (5 weeks old) were purchased from Beijing Vital River Bioscience (Beijing, China). All the animal care and experimental procedures were approved by the Institutional Animal Use and Care Committee of Huazhong University of Science and Technology and were performed according to the established guidelines. The study complied with all the relevant ethical regulations on animal research.

For the tumor growth studies, 5×10^6 A498 cells were injected subcutaneously into the flank of mice. Each group contained five mice. Tumor size was measured every three days. Finally, after four weeks, the mice were sacrificed, and the weight and volume of the tumors were assessed.

Cell culture and transient transfection of SLC17A9

The normal control cells HK2 and three ccRCC cell lines (786-O, A498, and CAKI-1) were purchased from the AmericanType Culture Collection (ATCC, USA), while OSRC-2 was purchased from the National Infrastructure of Cell Line Resource (NICR, China). HK2 is derived from human renal proximal tubular epithelial cells and is usually used as a control in renal cancer studies. 786-O is derived from primary ccRCC. A498 cells were isolated by Aaronson S from the kidney tissue of a 52-year-old woman kidney patient. CAKI-1 cell lines are skin metastatic cells of human ccRCC. OSRC-2 are renal cancer cells derived from a Japanese cancer patient. All the cells were cultured according to the methods previously described.[47] High glucose Dulbecco's Modified Eagle's Medium (DMEM; Gibco, USA) containing 10% fetal bovine serum (FBS; Gibco, USA) and 1% penicillin-streptomycin solution (Servicebio, China) were used to culture all the above cells. A stable humidified atmosphere with 5% CO_2 at 37 °C was used for cell incubation. Small interfering RNA (siRNA) specifically aiming for SLC17A9 and negative control were synthesized by GenePharma (Shanghai, China). Similarly, two siPTHLH were also purchased from GenePharma. The plasmids for SLC17A9 overexpression and negative control were designed by GeneChem (Shanghai, China). When the density of cancer cells in the 6-well plate reached about 70%, 3 μg of plasmid or siRNA and 5 μL of Lipofectamine® 2000 reagent (Thermo Fisher Scientific) were added to the medium. Cells were then collected after 72 h for the subsequent experiments. SLC17A9-specific overexpression plasmids and helper plasmids were transiently co-transfected into highly transfectable 293 T cells to produce high-titer lentivirus.[48] The lentiviral transduction system contained 25 μL of the transfection reagent A/P (Genechem, China) and 40 MOI lentivirus.

METHOD DETAILS

Clinical tissues collection

All the human ccRCC samples (n = 18) and adjacent kidney tissues (n = 18) were collected from the Department of Urology, Union Hospital, Tongji Medical College during 2019–2021. The detailed clinical information of all the patients including sex, age, and clinical-pathological information is presented in Table S1. All the participants had given informed consent, and the subject was approved by the Institutional Review Board of Huazhong University of Science and Technology, in compliance with Helsinki Declaration.

RNA extraction and qRT-PCR experiments

TRizol reagent (Thermo Fisher Scientific, Inc., Waltham, MA, USA) was used to extract the total RNA of tissue and cell samples. NanoDrop 2000 spectrophotometer (NanoDrop Technologies, Wilmington, USA) was used for measuring the concentration and purity of RNA. One μg RNA was reverse transcribed into cDNA. All the qRT-PCR analyses were conducted using the SYBR Green mix (Yeasen Biotech, Shanghai, China). Normalized formula: $2^{-\Delta Ct}$ ($\Delta Ct = Ct_{SLC17A9} - Ct_{GAPDH}$) was used to calculate the relative mRNA levels of SLC17A9. All the protocols followed were according to the manufacturer's instructions as previously described.[49] Specific primers were acquired from Sangon (Sangon, Wuhan, China).

Cell proliferation array

786-O and A498 cells transfected with siRNA or plasmids were seeded in 96-well plates with a density of 2×10^3/cells after 48 h. After the addition of CCK-8 reagent to the plates and incubation for 2 hat 37 °C, optical density (OD) values were measured at 450 nm.

Migratory and invasion assays

After incubating the transfected cells with serum-free DMEM medium for 24 h, the cells were cultured in a 24-well plate with the serum-free medium as the upper layer and serum-containing medium as the lower layer. The membrane was first incubated with Matrigel (Thermo Fisher Scientific) in the invasion assays. After 24 h of incubation, 100% methanol was added to fix cells and 0.05% crystal violet was used to stain them. A light microscope (Olympus CX41-32C02; Olympus Corporation, Tokyo, Japan) was used for determining the cell numbers and taking photos.

Immunohistochemistry (IHC) arrays

The tissues were fixed with formalin and dehydrated and then embedded with paraffin. Next, the sections were incubated with rabbit SLC17A9 primary antibody (1:100; 26731-1-AP; Proteintech, USA) at 4 °C overnight. The slices were washed three times with PBS and then incubated with goat anti-rabbit secondary antibody (1:200; GB23303; Servicebio, Inc., Woburn, MA, USA).

Western blotting (WB)

The tissues or cells were lysed to obtain protein samples using lysis buffer mixed with RIPA (Beyotime Institute of Biotechnology, Shanghai, China), PMSF (Wuhan Boster Biological Technology, Ltd.), and cocktail protease inhibitors (Roche Diagnostics, Indianapolis, IN, USA). 30 μg protein sample was added to 10% SDS-PAGE and separated at a stable voltage of 90 V. Then, the protein was transferred into polyvinylidene fluoride (PVDF) membranes (EMD Millipore, Billerica, MA, USA) at a stable current of 250 mA for 105 min. After being blocked in 5% milk for 1.5 hat room temperature, the transferred PVDF membranes were incubated with primary antibodies against SLC17A9 (1:1000; Proteintech, USA), Snail (1:1000, ABclonal), E-cadherin (1:1000, ABclonal), vimentin (1:1000, ABclonal), and β-actin (1:1000, Proteintech) at 4 °C overnight. Next, the membranes were incubated using secondary antibodies (1:10,000; BA1020; Wuhan Boster Biological Technology Ltd.) at room temperature for 2 h. Lastly, ChemiDoc-XRS+ (Bio-Rad Laboratories Inc., Hercules, CA, USA) was used for the detection of protein levels.

Bioinformatics analysis

The RNA expression matrix and clinical data were obtained from the TCGA database (n = 522) and the ICGC website (n = 136). R software and packages ("rms", "foreign", and "survival") were used to build prognostic nomogram models and calculate the c-index.[50] Time-dependent ROC curves were plotted using the "timeROC" package. Gene set enrichment analysis (GSEA) was conducted to obtain potential pathways involving SLC17A9. For the enriched pathways, the false discovery rate (FDR) < 0.25 and the p < 0.05

were considered statistically significant after carrying out 1000 permutations.[51] EMT-involved core hallmark gene sets were downloaded from GSEA software. CellMiner database, "limma", "ggplot2", and "impute" packages were used to calculate the correlations between SLC17A9 mRNA expression and IC_{50} of 161 drugs approved by the FDA.[52] The correlation analyses of SLC17A9 and EMT-related markers were performed by a Spearman method using GraphPad Prism 8. All the immune-related results were analyzed using CAMOIP according to the guidelines provided on its website.[25] All 522 samples of KIRC were initially divided into two groups according to the median expression of SLC17A9, and the "limma" package was then used to obtain the differential expressed genes (DEGs) related to SLC17A9, with adjusted $p < 0.05$ and $\log_2|FC| > 1$.

QUANTIFICATION AND STATISTICAL ANALYSES

Paired Student's ttest was used to analyze paired data, while a one-way ANOVA or t-test was used to analyze unpaired data. Survival analyses of patients based on SLC17A9 expression were presented by Kaplan-Meier (KM) curves for which the p value was calculated using the logrank test. The prognostic significance of SLC17A9 on OS and DFS of ccRCC patients was conducted by univariate and multivariate Cox proportional hazard regression using SPSS Statistics 23.0 (IBM Corporation, Armonk NY, USA), with $p < 0.05$ considered statistically significant.